International Journal of Electronics

Publication details, including instructions for authors and subscription information:
http://www.tandfonline.com/loi/tetn20

Monte Carlo calculation of velocity-field characteristics in II-VI compound semiconductors

A. DUTTA P. S. MALLICK D. MUKHOPADHYAY

Published online: 10 Nov 2010.

To cite this article: A. DUTTA P. S. MALLICK D. MUKHOPADHYAY (1998) Monte Carlo calculation of velocity-field characteristics in II-VI compound semiconductors, International Journal of Electronics, 84:3, 203-214, DOI: 10.1080/002072198134797

To link to this article: http://dx.doi.org/10.1080/002072198134797

INT. J. ELECTRONICS, 1998, VOL. 84, NO. 3, 203–214

Monte Carlo calculation of velocity-field characteristics in II–VI compound semiconductors

A. DUTTA†, P. S. MALLICK† and D. MUKHOPADHYAY†

The velocity field characteristics of II–VI compound semiconductors at 77 K have been obtained by the Monte Carlo simulation technique. The results agree with the available experimental data and with those obtained by solving the Boltzmann Transport Equation analytically. The simulation technique is described in detail and various aspects regarding the convergence of the simulation are discussed. The carrier distribution function has also been obtained from the simulation. The effects of the various simulation parameters, as well as those of the ionized impurity concentration, on the mobility values for the different semiconductors are discussed and results are presented.

1. Introduction

In recent times, the Monte Carlo simulation technique has been extensively used for the calculation of electrical conductivity characteristics in semiconductors. In this technique, the motion of the carrier inside the semiconductor under the influence of an applied electric field is simulated in a computer through the use of random numbers. A single carrier is followed through a large number of two-step, free flight-collision interaction cycles until finally the time average of any of the estimators used to characterize the motion reaches a steady state that is not evolving any further with time. Under such a condition, the ergodicity of the process can be invoked to describe the motion of the carrier ensemble from the study of the motion of the single carrier over a sufficiently long time. This ensures that both the spatial and temporal stabilization of the energy distribution function of the carriers have been achieved and the computed time average of the estimator actually represents the true average value of the corresponding physical quantity.

The analytical methods for obtaining the conduction properties in semiconductors involving the solution of the Boltzmann transport equation (BTE) under a large applied electric field condition is beset with many complications. Under high field conditions, the important scattering mechanisms in compound semiconductors are neither elastic nor randomizing and the usual relaxation time approximation cannot be used for solving the BTE. Various approximations, not all of which can be justified, have been used to obviate this difficulty under high-field conditions. The Monte Carlo technique provides a better and more rigorous solution in such a situation. This being a simulation process, no attempt is made to solve the BTE, nor is the energy distribution function of the carriers approximated by any simplified and analytically manageable function. This technique has been extensively used to obtain the velocity–field characteristics of III–V compound semiconductors (Fawcett *et al.*, 1970). The velocity-field characteristics of II–VI compound semiconductors, on the other hand, have not been studied systematically or in any great detail using

Received April 1997; accepted 27 May 1997.

† Device Modelling Laboratory, Department of Electronics and Telecommuncation Engineering, Jadavpur University, Calcutta-700 032, India.

0020–7217/98 $12.00

the Monte Carlo technique. We present in this paper, the detailed Monte Carlo technique for obtaining the velocity–field characteristics in some of the II–VI compound semiconductors like ZnO, ZnS, CdS, CdSe and CdTe.

Section 2 describes the approximations used for incorporating the non-parabolicity of the band structure in the simulation. Section 3 gives the calculation of the rates of the different scattering processes involved. Section 4 describes the Monte Carlo simulation technique and discusses the various aspects regarding the convergence of the simulation, the accuracy and reproducibility of the estimator and computer time involved. Finally, in § 5, we present the results on electron mobility in the different II–VI compound semiconductors and discussions thereof.

2. Band structure and dispersion relation

The II–VI compound semiconductors discussed here are large bandgap materials with a direct bandgap. The minimum of the conduction band is situated at the centre of the Brillouin zone and the other subsidiary minima in the conduction band are so far removed in energy from the central conduction band minimum that their effect on the velocity–field characteristics can be neglected in the field range considered here. The non-parabolicity of the conduction band is also not very pronounced, because of the large energy bandgaps.

For the semiconductors considered here, we have assumed a simple non-parabolic band structure such that the E–k relationship is given by (Nag 1980)

$$\gamma(\mathrm{E}) = \frac{\hbar^2 \mathrm{k}^2}{2\mathrm{m}^*}$$

where

$$\gamma(\mathrm{E}) = \mathrm{E}(1 + \alpha\mathrm{E})$$

$$\alpha = \frac{1}{\mathrm{E_g}}\left(1 - \frac{\mathrm{m}^*}{\mathrm{m_0}}\right)^2\left(1 - \frac{\mathrm{E_g}\Delta}{3(\mathrm{E_g} + \frac{2}{3}\Delta)(\mathrm{E_g} + \Delta)}\right)$$

In the above approximation the relations—namely (i) E as a function of $\boldsymbol{k}$; (ii) $\boldsymbol{k}$ as a function of E; and (iii) $\partial\gamma/\partial E$ as a function of E—are explicit and hence their incorporation in a Monte Carlo program is straightforward.

3. Scattering rates

The free flight of a carrier through the lattice is disturbed by collisions with lattice vibrations and impurity atoms. Let, at an instant of time t, the wave vector of the carrier be $\boldsymbol{k}$. If the carrier suffers a collision at time t its wave vector changes from $\boldsymbol{k}$ to $\boldsymbol{k}'$.

The scatterings that have been considered here are scattering by ionized impurity atoms, by polar optical phonons and by acoustic phonons through deformation potential coupling and through piezoelectric interaction.

Each of these collisions is characterized by the scattering rate $S_i(\boldsymbol{k})$ which is the number of collisions of type i per unit time per unit volume in the $\boldsymbol{k}$ space.

$$\mathrm{S_i}(\boldsymbol{k}) = \frac{\mathrm{V_c}}{8\pi^3}\int \frac{2\pi}{\hbar}\left|\mathrm{M_i}(\boldsymbol{k}, \boldsymbol{k}')\right|^2 \delta(\mathrm{E}_{\boldsymbol{k}} - \mathrm{E}_{\boldsymbol{k}'})\,\mathrm{d}\boldsymbol{k}' \qquad (1)$$

where V_c is the crystal volume.

$M_i(\boldsymbol{k},\boldsymbol{k}')$ is the matrix element for the ith scattering mechanism for scattering from the $\boldsymbol{k}$ state to the $\boldsymbol{k}'$ state, and may be written as

$$|M_i(\boldsymbol{k},\boldsymbol{k}')| = [A_i(|\boldsymbol{k}-\boldsymbol{k}'|)]G(\boldsymbol{k},\boldsymbol{k}')$$

$G(\boldsymbol{k},\boldsymbol{k}')$ is the overlap function, an A_i is the matrix element without the overlap function and is given, for the different scattering mechanisms, by (Nag 1980)

$$A_{imp} = \frac{Ze^2}{V_c\varepsilon}\frac{1}{|k-k'|^2+\lambda^{-2}}$$

$$A_{ao} = E_l\left(\frac{\hbar}{2V_c\rho\omega_q}\right)^{1/2}(e_q\cdot q)S_c(q,\lambda)(n_q+\tfrac{1}{2}\pm\tfrac{1}{2})^{1/2}$$

$$A_{pz} = \frac{|e|h_{pz}}{\varepsilon}\left(\frac{\hbar}{2V_c\rho\omega_q}\right)^{1/2}S_c(q,\lambda)(n_q+\tfrac{1}{2}\pm\tfrac{1}{2})^{1/2}$$

$$A_{pop} = \frac{|e|}{q}\left(\frac{1}{\kappa_\alpha}-\frac{1}{\kappa_0}\right)\left(\frac{\hbar\omega_l}{2V_c\varepsilon_0}\right)^{1/2}S_c(q,\lambda)(n_q+\tfrac{1}{2}\pm\tfrac{1}{2})^{1/2}$$

where λ is the Debye screening length, E_l is the acoustic phonon deformation potential coupling constant, h_{pz} is the piezoelectric constant, ω_l is the longitudinal polar optical phonon frequency, $q = |\boldsymbol{k}-\boldsymbol{k}'|$, Z is the ionicity of an impurity atoms, assumed unity and

$$S_c(q,\lambda) = \frac{q^2}{q^2+\lambda^{-2}} \text{ is the screening factor}$$

Substituting the appropriate matrix element, we get the rates of the different scattering processes as follows.

3.1. *Ionized impurity scattering*

$$S_{imp}(\boldsymbol{k}) = C_{imp}F_{imp}(\boldsymbol{k},\lambda)\gamma'(E_{\boldsymbol{k}})k^{-3} \tag{2}$$

where

$$C_{imp} = \frac{Z^2e^4N_im^*}{8\pi\varepsilon^2\hbar^3}$$

$$F_{imp}(\boldsymbol{k},\lambda) = 2\left[\frac{(a+be+ce^2)}{e^2-1}+c\right]-(b+2ce)\ln\left(\frac{e+1}{e-1}\right)$$

where

$$e = 1+\frac{1}{2k^2\lambda^2}$$

3.2. *Polar optical phonon scattering*

$$S_{pop}(\boldsymbol{k},\lambda) = \frac{e^2\omega_l\left(\frac{1}{\kappa_\alpha}-\frac{1}{\kappa_0}\right)}{8\pi^2\varepsilon_0}\sum_{+,-}\int\frac{|\boldsymbol{k}-\boldsymbol{k}'|^2G(\boldsymbol{k},\boldsymbol{k}')}{[|\boldsymbol{k}-\boldsymbol{k}'|^2+\lambda^{-2}]}(n_l+\tfrac{1}{2}\pm\tfrac{1}{2})\delta(E_{\boldsymbol{k}}-E_{\boldsymbol{k}'}\pm\hbar\omega_l)\,d\boldsymbol{k}' \tag{3}$$

where

$$n_l = \frac{1}{\exp\left(\frac{\Theta_D}{T_L}\right)-1}$$

Using the property of the δ function, substituting for $d\boldsymbol{k}'$ and integrating over the entire k-space, we get

$$S_{pop}(\boldsymbol{k},\lambda) = C_{pop}\left(\frac{1}{\boldsymbol{k}^2}\right) \sum_{+,-} k_{\pm} F_{pop}(\boldsymbol{k},\lambda)\gamma'(E_{\boldsymbol{k}} \pm \hbar\omega_l)(n_l + \tfrac{1}{2} \pm \tfrac{1}{2})$$

where $\boldsymbol{k}_{\pm}$ are the wave vectors corresponding to $E_{\boldsymbol{k}} \pm \hbar\omega_l$

$$C_{pop} = \frac{e^2\omega_l m^*}{4\pi\varepsilon_0\hbar}\left(\frac{1}{\kappa_\alpha} - \frac{1}{\kappa_0}\right)$$

$$F_{pop} = \frac{1}{4f^2}\left[4af^2 + 2bf(g + 2d) + cg(g + 4d)\right]\ln\left(\frac{g + 2f}{g - 2f}\right) - \frac{1}{f}\left[2bf + c(g + 2d) + \frac{2df\{4f(a + c) + 2bg\}}{g^2 - 4f^2}\right]$$

where $f = k_{\pm}/k$, $g = 1 + f^2 + 2d$.

3.3. *Acoustic phonon scattering*

$$S_{ac}(\boldsymbol{k},\lambda) = \frac{E_l^2 K_B T_L}{4\pi^2\rho\hbar s^2}\int \frac{|\boldsymbol{k} - \boldsymbol{k}'|^2 G(\boldsymbol{k},\boldsymbol{k}')}{\left[|\boldsymbol{k} - \boldsymbol{k}'|^2 + \lambda^{-2}\right]}\delta(E_{\boldsymbol{k}} - E_{\boldsymbol{k}'})\,d\boldsymbol{k}'$$

$$= C_{ac}F_{ac}(\boldsymbol{k},\lambda)\gamma'(E_{\boldsymbol{k}}) \qquad (4)$$

$$C_{ac} = \frac{E_l^2 K_B T_L m^*}{\pi\rho\hbar^3 s^2}$$

$$F_{ac} = a + \frac{c}{3} + 2bd + 2cde + \frac{d(a + be + ce^2)}{e + 1} - (ad + be + 2cde^2 + \tfrac{1}{2}bd^2)\ln\left(\frac{e + 1}{e - 1}\right)$$

3.4. *Piezoelectric phonon scattering*

$$S_{pz}(\boldsymbol{k},\lambda) = \frac{e^2\hbar_{pz}^2}{8\pi^2\varepsilon^2\rho s^2}\int \frac{|\boldsymbol{k} - \boldsymbol{k}'|^2\omega_q}{\left[|\boldsymbol{k} - \boldsymbol{k}'|^2 + \lambda^{-2}\right]} G(\boldsymbol{k},\boldsymbol{k}')\delta(E_{\boldsymbol{k}} - E_{\boldsymbol{k}'} \pm \hbar\omega_l)(n_q + \tfrac{1}{2} \pm \tfrac{1}{2})\,d\boldsymbol{k}'$$

$$= C_{pz}F_{pz}(\boldsymbol{k},\lambda)\gamma'(E_{\boldsymbol{k}})\left|\frac{1}{\boldsymbol{k}}\right| \qquad (5)$$

$$C_{pz} = \frac{e^2\hbar_{pz}^2 K_B T_L m^*}{2\pi\rho\hbar^3 s^2\varepsilon^2}$$

$$F_{pz} = \left(c - b - 2ce + \frac{a + be + ce^2}{e + 1}\right) - (a + be + ce^2 + 2cde)\ln\left(\frac{e + 1}{e - 1}\right)$$

The variation of the various scattering rates with energy in CdS at 77 K is shown in Fig. 1 together with the variation of the total scattering rate for an ionized impurity concentration of 10^{15} cm^{-3}. It is to be noted that, in Monte Carlo calculations, the polar optical phonon emission and absorption are treated as two separate

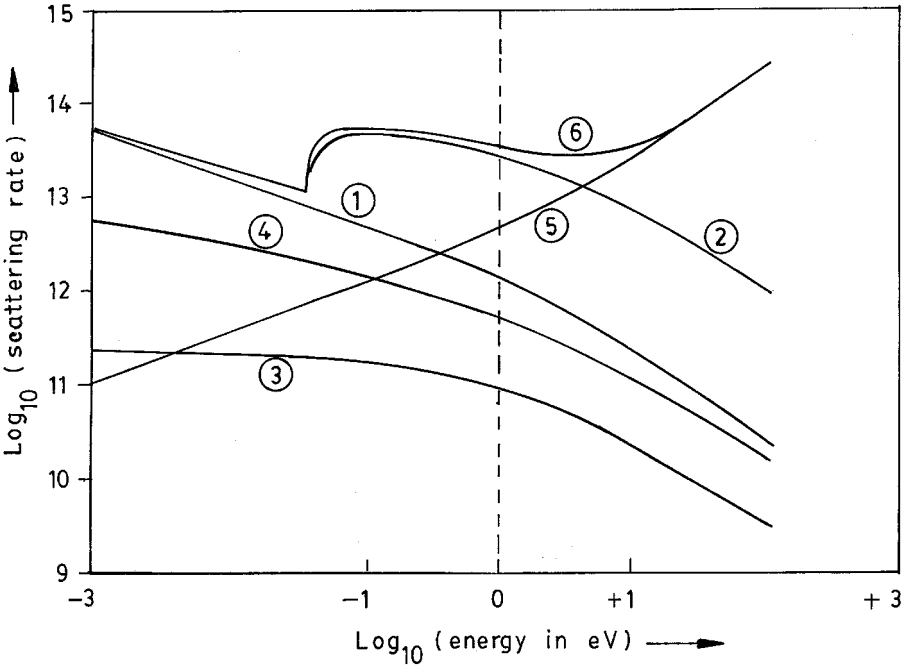

Figure 1. Variation of the various scattering rates with energy in CdS at 77 K together with the variation of the total scattering rate for an ionized impurity concentration of 10^{15} cm^{-3}: (1) P.O. Abs.; (2) P.O. Emi.; (3) impurity; (4) piezo; (5) acoustic; (6) total.

processes. It is found that the total scattering rate decreases rapidly with energy up to the optical phonon energy when optical phonon emission takes place, and the total scattering rate increases at this energy. The total scattering rate then decreases as all the scattering rates (except that for acoustic phonons) are, in general, decreasing functions of energy. Above an energy of about 3 eV the total scattering rate, however, increases with energy due to increasing occurrence of acoustic phonon scattering. In an actual simulation a maximum energy value is chosen such that the electron energy almost never reaches that high value and the Rees' parameter, Γ, is taken to be the total scattering rate at that chosen maximum energy. This choice obviously requires an *a priori* knowledge of this variation of the total scattering rate with energy in the material. The type of variation of the total scattering rate as described above is characteristic of the II–VI compound semiconductors and is the same for all the semiconductors considered here.

4. The Monte Carlo simulation procedure

The carrier is presumed to start with an initial wave vector $\boldsymbol{k}_0$. Under the influence of the external electric field, it accelerates and continues its motion in what is called its free flight. The duration of this free flight is estimated by a (pseudo) random number r_0 distributed uniformly between 0 and 1. The time at which the collision takes place is given by

$$t_c = -(\ln r_0)/\Gamma \tag{6}$$

where Γ is the chosen Rees' parameter. Γ has been rendered constant over the energy range considered by including a self-scattering term such that the sum of all the real scattering rates plus the self-scattering rate remains constant over the entire energy range considered. It has been shown that the steady-state value obtained by including the self-scattering term is indeed the value corresponding to the real scatterings (Rees 1969). The wave vector of the carrier at the end of the free flight is $\boldsymbol{k}$ and this is computed using the laws of classical mechanics.

Once t_c is determined, one may plot the trajectory of the electron from 0 to t_c by using the laws of newtonian mechanics. Thus

$$x = (\hbar/m^*)k_{x0}(t_c - t_0)$$
$$y = (\hbar/m^*)k_{y0}(t_c - t_0)$$
$$z = (\hbar/m^*)\left[k_{z0}(t_c - t_0) + (eE/2\hbar)(t_c - t_0)^2\right]$$

where k_{x0}, k_{y0}, k_{z0}, are the x, y and z components of k_0 at $t = t_0$, and the polar axis z has been chosen as the direction of the applied field.

Having determined the instant at which the free flight has terminated, we now have to determine the type of collision that has terminated the free flight. The various scattering rates S_i corresponding to the various scattering mechanisms for the carrier with wave vector $\boldsymbol{k}$ are computed by using the equations as detailed earlier. Next, another random number r_1 is used to ascertain which one of the n scattering mechanisms, including the self-scattering process, has been operative. The jth mechanism is chosen to terminate the free flight, if

$$\frac{\sum_{i=1}^{j} S_i}{\sum_{i=1}^{n} S_i} \leqslant r_1 < \frac{\sum_{i=1}^{j+1} S_i}{\sum_{i=1}^{n} S_i} \tag{7}$$

Having determined the kind of scattering, the energy and the wave vector of the electron after a real collision are determined from the conservation of the energy and the momentum. The energy of the electron after collision is given by $E + \Delta E$, where ΔE is the change in energy induced by the collision and E is the energy of the electron immediately before the collision. It is given by

$$E = \hbar^2 k^2(t_c)/2m^*$$

For acoustic, piezoelectric and ionized impurity scatterings ΔE is taken equal to zero while for polar optical phonon scattering it is equal to $\hbar\omega_l$.

The magnitude of the electron wave vector after the collision is then given by

$$k_i = \left[2m^*(E + \Delta E)\right]^{/2}/\hbar \tag{8}$$

This value of the wave vector is taken as the initial wave vector for the next free flight.

The orientation of the wave vector after collision is obtained by generating two more random numbers r_2 and r_3, distributed uniformly between 0 and 1. We note that the probability that the polar angle θ, and the azimuthal angle ϕ of the wave vector $\boldsymbol{k}_i$ with respect to any convenient directions, will be contained in the intervals

$d\theta$ and $d\phi$ is proportional to $\sin\theta\, d\theta\, d\phi$. θ and ϕ can, therefore, be chosen with the random numbers r_2 and r_3 as

$$\cos\theta = 1 - 2r_2 \tag{9}$$

$$\phi = 2\pi r_3 \tag{10}$$

The distribution function of the electrons can be obtained from the results of these computations. For this purpose the entire $\boldsymbol{k}$ space is subdivided into a large number of cells and the time the electron spends in a particular cell of the $\boldsymbol{k}$ space is logged and the value is normalized by the total time. This gives the probability of the electron being in that cell, and hence the distribution function. In arriving at this calculation our argument is based on the ergodic theorem which states that the ensemble average for a particular variable is the same as the time average of the same variable for a single particle, provided it is observed over a sufficiently long time. The distribution function thus obtained is shown in Fig. 2 for CdS at 77 K for applied electric fields of 5 and 10 kV cm^{-1} for zero ionized impurity concentration.

The average velocity can be obtained from displacement and time by dividing the total displacement along the field direction by the total time.

$$v_z = (\hbar/m^*) \sum_i \left(k_{z0} t_{ci} + (eE/\hbar)(t_{ci}^2/2) \right) \sum_i t_{ci} \tag{11}$$

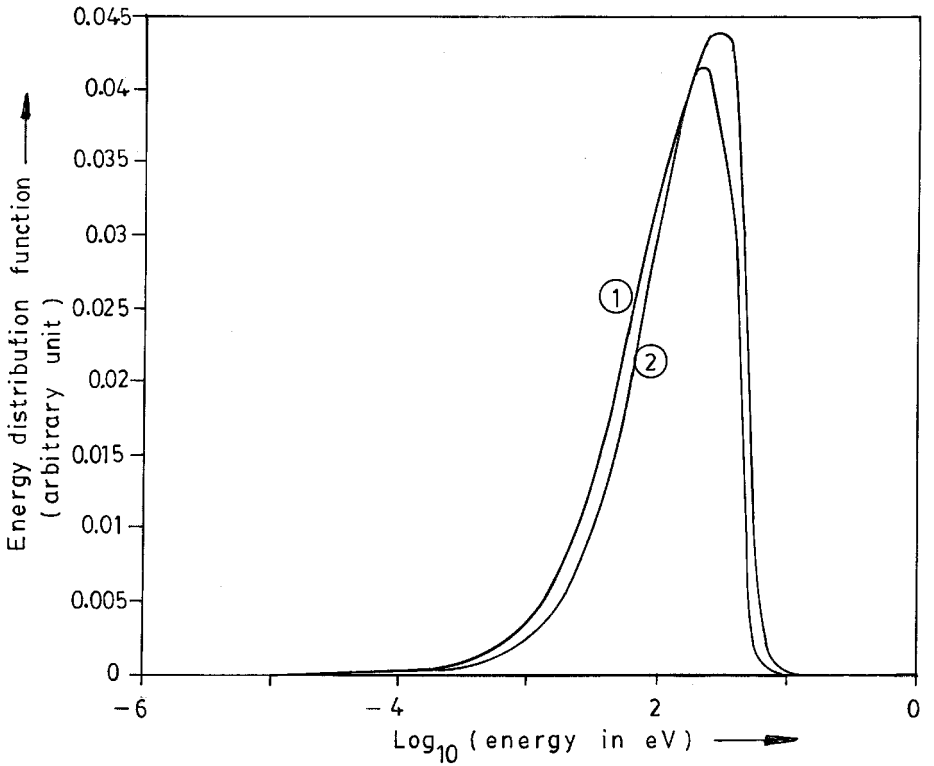

Figure 2. The distribution function for CdS at 77 K for applied electric fields of 5 and 10 kV cm^{-1} for zero ionized impurity concentration. (1) 5 kV cm^{-1}; (2) 10 kV cm^{-1}.

The average velocity can also be obtained from the energy and momentum by using the relation (Nag 1980)

$$v_d = \hbar^{-1} \sum (E_f - E_i) \Big/ \sum (k_{fz} - k_{iz}) \tag{12}$$

where E_i and E_f are, respectively, the energy after a collision and before the next collision. k_{iz} and k_{fz} are the corresponding components of the wave vector in the field direction.

It may be noted that calculation of velocity by this method is not possible at low fields as the unbalanced part of the random velocities could be comparable to the drift velocity. To avoid this difficulty, low field mobility is evaluated in the Monte Carlo simulation indirectly through the diffusion constant by using the Einstein relation. It is to be noted that the velocity values obtained by using the above two methods agree exactly with each other.

4.1. *Convergence and termination of the simulation*

In any simulation procedure for a stochastic process, the convergence of the estimator value and its confidence limit at the termination of the simulation procedure, pose the single most important question to be answered. Usually and almost tentatively, it is said that the simulation procedure should cover a large number of events. But how large should this number be? With modern day high speed processors, one can go on calculating the electron trajectories for say 100 000 events, i.e. 100 000 real collisions. But then the question remains, how much do we gain in terms of our confidence in the estimator value, the average velocity in this case, by extending the simulation beyond a certain point? There are several interesting aspects involved in this question, insight about which can be gained only by going through the experience of simulating the particular process. We discuss some of the more important of these points below.

We know that the total scattering rate S_T of the electron is a function of energy, $S_T(E)$. Since we are not in a position to generate a random number which exactly matches this distribution of $S_T(E)$ over energy, we have to introduce a new fictitious 'self-scattering' such that the total scattering rate, including this 'self-scattering' is constant and equal to the Rees' parameter Γ. This enables us to proceed with the simulation by generating uniformly distributed random numbers.

We note that, in general, the total scattering rate $S_T(E)$ is simply a function of the electron energy, $S(E)$, and Γ should be larger than the largest value of $S_T(E)$. We can, therefore, set an arbitrary large value of Γ for the simulation. This, however, increases the number of self-scatterings, resulting in an unnecessary increase in the computation time. It has been observed during our calculations that the computation time increases almost linearly with the value of Γ. A suitable choice for Γ is then the maximum value of $S_T(E)$ in the region of energies that are expected to be sampled during the simulation. Often $S_T(E)$ is an increasing function of E, particularly in the high energy range, due to the contribution of acoustic phonon scattering. In such a case, one can take $\Gamma = S_T(E_M)$, where E_M is the maximum electron energy with negligible probability of being achieved by the electron during the simulation. This is illustrated in Fig. 1 in which we have plotted the variation of the total scattering rate with energy in CdS at 77 K for $N_i = 1 \times 10^{15}$ cm^{-3}. E_m is the max-

imum energy that may be reached by the electron during the simulation and the value of the Rees' parameter is taken to be equal to $S_T(E_M)$.

It must be observed, however, that the range of energy visited by the electron during the simulation is not known at the beginning, when Γ is to be chosen. Therefore, an estimate must be made for E_M keeping in mind that E_M cannot be taken as too large, if one is to prevent a waste of computer time by self-scattering events.

In our scheme, we first have a trial run for a particular situation. We also introduce the concept of 'missed collision', which is a complementary concept of 'self-collision' and occurs when Γ is too small. A small value of Γ forces the electron to continue in its simulated motion without undergoing a collision when, in fact, it should have undergone a collision by then. We say that the electron has a missed collision whenever its energy is larger than E_M, when Γ has been chosen such that $\Gamma = S_T(E_M)$. In our test procedure we keep a log of the minimum, the maximum, the average and the standard deviation of the values of electron energy and the total scattering rate. We also keep a record of the number of missed collisions for the particular choice of Γ. If the number of missed collision is more than 1 in 10^4 real collisions, we increase the value of Γ until the number of missed collision is less than 1 in 10^4 real collisions. This ends the test run and, from the energy and scattering rate records, we choose Γ for the actual simulation in such a way that it satisfies both the following conditions

$$\Gamma \geqslant S_T(E_M + 2\delta_E)$$

$$\Gamma \geqslant S_{T\,max} + 2\delta_{ST}$$

where δ_E and δ_{ST} are, respectively, the standard deviation of energy and total scattering rate and E_M and $S_{T\,max}$ are, respectively, their maximum values.

Having fixed the choice of Γ for a particular situation from the test run, we begin our simulation procedure keeping a record of the missed collisions and the maximum, minimum and standard deviation values of the energy and total scattering rate. Whenever a missed collision occurs, the simulation stops automatically after printing all the results in an output file. The current value of the seed of the random number generator is also preserved. If the estimator value, the drift velocity, has not shown sufficient convergence at this point, the simulation is extended further with a 10% increase in the value of Γ and by taking the preserved seed of the random number generator as the new seed.

An important point needs be noted in this context. Theoretically, the value of the drift velocity should not depend upon the value of Γ provided a very large number of events (electron trajectories) have been considered. It has, however, been observed that in an actual simulation, the final value of the drift velocity shows a very weak dependence upon the choice of Γ. In our calculation it is observed that the electron mobility in CdS at 77 K for an applied electric field of 10 kV cm^{-1} and zero ionized impurity concentration varies by about 2% when the Rees' parameter Γ changes by two orders of magnitude, provided there is no missed collision in that range of Γ. The simulation was carried for 100 000 real collisions for each value of Γ.

The convergence of the estimator value poses another problem in this simulated study, because essentially we are studying a problem that is stochastic in nature. The problem becomes accentuated because of the slow rate of convergence of the estimator value. Different authors have used different convergence tests. Some of these,

based on the testing of two individual events, could be quite misleading particularly when elastic collisions are involved. To apply a test for convergence, we have, first of all, considered only a real collision as an event; self scatterings have been left out as 'non-events' since they do not change the momentum or energy of the moving electron. Then, the entire history of events has been subdivided into a number of sub-histories. A sub-history, in our case, consists of 1000 real collisions. The estimator value is supposed to have converged when the average and the standard deviation of the estimator value for ten such sub histories differ by less than 1% from the corresponding quantities for the immediately preceding ten sub histories. Based on observations for the simulation, it is found that convergence is obtained normally between 50 000 to 100 000 real collisions depending upon the applied electric field and, more importantly, upon the material chosen. It is observed that convergence is rather slow for II–VI compound semiconductors, particularly CdS.

5. Results and discussions

The model for Monte Carlo simulation described earlier is implemented in C. The software incorporates a data table containing the various physical parameters of the materials, shown in Table 1. Formulations for computation of different band properties, such as overlap integral, $\partial\gamma/\partial E$ etc are included in the program. Also included are scattering rate computation routines for various scattering processes. To run the simulation, the name of the material, the lattice temperature, the impurity concentration, the applied electric field and which of the scattering processes are to be considered (by default all the processes are assumed to be operative) and the simulation parameter Γ, need be supplied. The simulation is found to converge after between 50 and 100 000 real scatterings depending upon the applied electric field and the material considered. The simulation has been performed under fields ranging from 1 kV cm^{-1} to 50 kV cm^{-1} depending upon the particular semiconductor and lattice temperature. The materials investigated are ZnO, ZnS, CdS, CdSe and CdTe. The calculated results agree to within 5% to 10% of the available experimental data and with calculations based on analytical techniques, such as the calculations using a displaced Maxwellian distribution function. As an example we note that for cadmium telluride at 77 K, the mobility obtained by Monte Carlo simulation is 2192.5 cm^2 V^{-1} s^{-1} while that obtained by solving the Boltzmann equation is 2122 cm^2 V^{-1} s^{-1} at a field of 7 kV cm^{-1} (Mukhopadhyay and Bhattacharya 1984). The experimental value of the mobility obtained by Canali *et al.* at this field is 2143 cm V^{-1} s^{-1} (Canali *et al.* 1971). At a field of 8.5 kV cm^{-1}, the corresponding values are 2214.4, 2202.5 and 2330 cm^2 V^{-1} s^{-1}, respectively.

Material	$\frac{m^*}{m_0}$	κ_0	κ_α	ρ g cm^{-3}	$s_1 \times 10^{-5}$ (cm s^{-1})	θ_D (K)	K_m^2	E_1 (eV)
ZnO	0.32	8.50	4.59	5.66	5.0	851	0.074	10
ZnS	0.28	8.90	5.14	4.08	5.0	507	0.074	10
CdS	0.15	9.19	5.24	4.80	4.3	440	0.037	12.8
CdSe	0.13	9.25	6.40	5.81	5.0	304	0.026	10
CdTe	0.10	9.60	7.21	6.06	3.0	242	0.068	18

Table 1. Material parameters used for numerical calculation of mobility values.

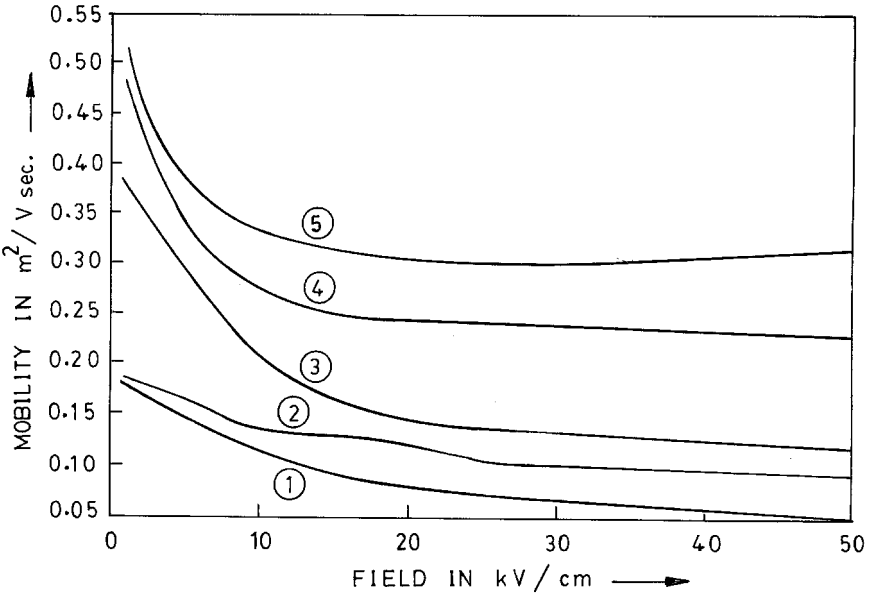

Figure 3. Variation of the electron mobility with the applied electric field for several II–VI compound semiconductors like ZnO, ZnS, CdS, CdSe and CdTe for an ionized impurity concentration of 10^{15} cm^{-3}. (1) ZnO; (2) ZnS; (3) CdTe; (4) CdS; (5) CdSe.

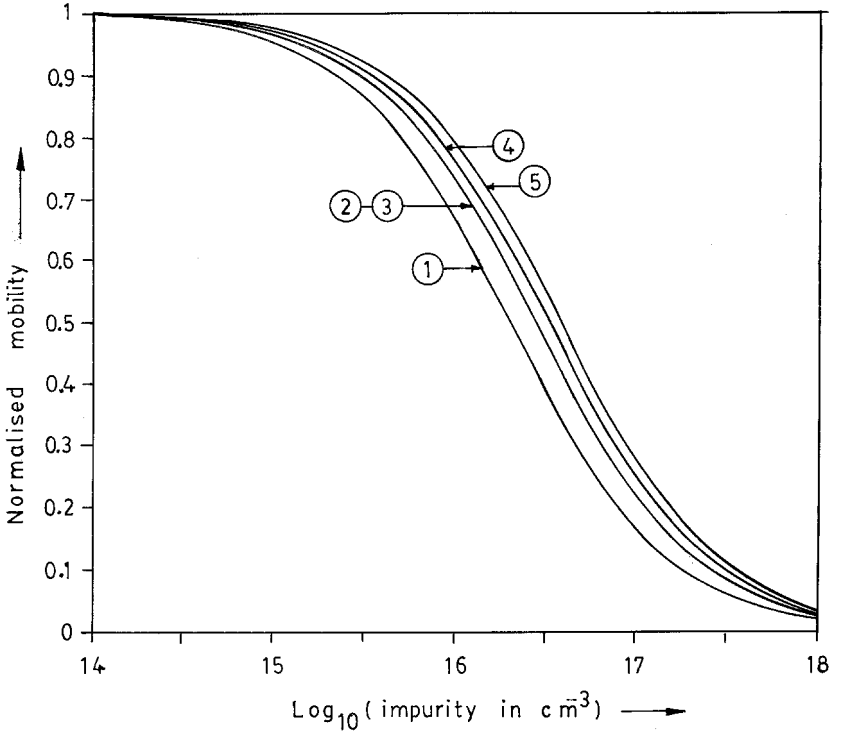

Figure 4. Variation of the normalized values of the low-field electron mobility at 77 K in the various II–VI compound semiconductors with the ionized impurity concentration. (1) CdS; (2) ZnO; (3) CdSe; (4) ZnS; (5) CdTe.

In Fig. 3, we have plotted the variation of the electron mobility with the applied electric field for several II–VI compound semiconductors like ZnO, ZnS, CdS, CdSe and CdTe for an ionized impurity concentration of 10^{15} cm^{-3} in each case. It is found that the mobility decreases monotonically with the applied electric field in all these semiconductors, as in elemental or in III-V compound semiconductors.

Figure 4 shows the variation with the ionized impurity concentration of the low-field electron mobility in the different semiconductors at 77 K. In this figure the low-field mobility values have been normalized by their corresponding values for a small ionized impurity concentration of 10^{14} cm^{-3}. It is found that for all the semiconductors considered here, the mobility values decrease with the ionized impurity concentration, slowly at first and then drastically for impurity concentrations in excess of 3×10^{15} cm^{-3}.

5.1. *Conclusions*

It has been generally described in the literature that the Rees' constant Γ should be chosen larger than the total scattering rate. But nothing definite has been prescribed that can guide one to choose Γ properly. The problem becomes all the more important because one has to choose the value of Γ before the simulation procedure begins. Usually, Γ is chosen arbitrarily large, which often leads to a large number of self-scatterings and a waste of computer time.

The concept of 'missed collisions', as has been introduced here, gives a quantitative estimate of Γ and leads to its proper choice. We conclude that Γ should be just as large so as not to allow any 'missed collisions'; any larger value of Γ than this only increases the computation time without having any considerable effect on the simulation process. The 'missed collisions' on the other hand, affect the simulation process and change the estimator value appreciably.

The fact that the convergence rate depends upon the semiconducting material chosen has neither been appreciated nor been explicitly stated in the literature. Our studies on various semiconductors show that the rate of convergence is much faster in some materials than in others. It is also found that the convergence is slower for higher ionized impurity concentration. This is because ionized impurity scatterings, being essentially elastic, randomize the distribution function and delay the convergence.

References

Canali, C., Martini, M., Ottaviani, G., and Zanio, K. R., 1971, Transport properties of CdTe. *Physical Review*, **B4**, 422–431.

Fawcett, W., Boardmann, A. D., and Swain, S., 1970, Monte Carlo determination of electron transport properties in gallium arsenide. *Journal of the Physics and Chemistry of Solids*, **31**, 1963–1990.

Mukhopadhyay, D., and Bhattacharya, D. P., 1984, Electron transport in II–VI compound semiconductors. *Journal of the Physics and Chemistry of Solids*, **45**, 393–399.

Nag, B. R., 1980, *Electron Transport in Compound Semiconductors*. Solid State Sciences Series, Vol. 11 (Berlin: Springer-Verlag).

Rees, H. D., 1969, Calculation of distribution function by exploiting the stability of the steady state. *Journal of the Physics and Chemistry of Solids*, **30**, 643–655.